

# Thermophoresis of Highly Absorbing, Emitting Particles Suspended in a Mixed Convection Flow System

혼합 대류 유동시스템에 부유된 고흡수 방사하는 입자의 열 확산

S. J. Yoa\*  
여 석 준

## 요 약

혼합 대류 이상 유동 시스템에 부유된 슈트와 미분탄과 같은 고흡수, 방사하는 입자의 열확산적 입자이동에 대한 복사 및 부력효과를 수치적으로 검토하였다. 기체 및 입자유동의 지배방정식들은 Euler 관점의 two-fluid model 의 근간에서 수행되었으며, 에너지 보존식의 비선형 복사 생성항은 P-1 근사방법에 의해 계산되었다. 혼합 대류 유동에서의 입자의 열확산현상은 복사 열전달과 커플링되며, 복사효과의 증가는 부력효과를 상대적으로 감소시켜 부력효과에 의한 입자 부착율을 완화시켰다. 복사효과가 무시될 때 Grashof 수의 증가에 따라 입자의 확산효과는 감소되었으며, 복사효과가 함께 작용될 때 입자 부착율은 증가됨을 보였다.

## Nomenclature

### Glossary symbols

$C_L$  Thermal loading ratio(=  $\rho_p C_{pp} / \rho_g C_{pg}$ )  
 $C_{pg}$  Heat capacity of gas  
 $C_{pp}$  Heat capacity of particle  
 $C_T$  Temperature jump coefficient  
 $D$  Tube diameter  
 $dp$  Particle diameter  
 $E(x)$  Cumulative collection efficiency defined by equation (18)  
 $G_0$  Dimensionless zeroth-order moment of intensity  
 $Gr$  Grashof number  
 $I_0$  Zeroth-order moment of intensity

$K$  Thermophoretic coefficient  
 $K_g$  Conductivity of the gas  
 $K_p$  Conductivity of the particle  
 $K_L$  Thermal slip coefficient  
 $N$  The ratio of conduction to radiation  
 $N_p$  Number of particles per unit volume  
 $Pe$  Peclet number(=  $RePr$ )  
 $Pe_r$  Peclet number(=  $Re_r Pr$ )  
 $Pr$  Prandtl number  
 $R$  Tube radiums  
 $Re$  Reynolds number(=  $U_{avg} D/v$ )  
 $Re_r$  Reynolds number(=  $U_{avg} D/v$ )  
 $Stk$  Stokes number  
 $T$  Temperature  
 $T_m$  Mixed mean temperature

\* 부산수산대학교 환경공학과

$u$	Velocity in axial direction
$U_{avg}$	Average velocity over the cross section in $x$ -direction
$v$	Velocity in vector form in radial direction
$v_T$	Thermophoretic velocity
$v_p$	Volume of single particle
$x$	Axial coordinate

## Greek character

$\alpha_T$	Thermal diffusion factor
$\beta$	Absorption coefficient
$\epsilon_p$	Particle surface emissivity
$\epsilon_w$	Tube surface emissivity
$\Phi$	Dimensionless particle concentration ratio ( $\rho_p/\rho_p, in$ )
$\eta$	Dimensionless radial coordinate
$\lambda$	Molecular mean free path
$\mu$	Dynamic viscosity of gas
$\nu$	Kinematic viscosity of gas
$\theta$	Dimensionless temperature ( $T/T_{in}$ )
$\theta^*$	$T_w/(T_{in}-T_w)$
$\rho_g$	Gas density
$\rho_p$	Apparent particle density
$\rho_{p, in}$	Apparent particle density at tube inlet
$\rho_{pm}$	Material density of single particle
$\sigma$	Stefan-Boltzmann constant
$\tau_o$	Optical thickness
$\zeta$	Dimensionless axial coordinate

## Subscript

$b$	refers to black body
$g$	refers to gas phase
$in$	refers to tube inlet
$p$	refers to particle phase
$w$	refers to wall surface

## Superscript

$R$	refers to radiation
-----	---------------------

\* refers to dimensionless form

## Introduction

Small particles such as dust, fly ash, and soot suspended in a gas stream with a temperature gradient, experience a force in the direction opposite to the temperature gradient[1]. This so called thermophoresis phenomenon is applied to the fabrication of optical wave guides, semi-conductor devices and the successful design of many types of equipment such as a heat exchanger.

Experimentally, thermophoretic transport of particles has been studied by Derjaguin et al. for particles up to about  $5\mu m$  in diameter, Goldsmith et al. for small particles and in a turbulent pipe flow by Calvert and Byers[2-6]. Additionally, it has been investigated by Goren, Epstein et al. in the channel flows and boundary layer flows over a flat plate and tube flows by Walker et al. numerically or analytically [7, 8]. Most of the workers for the analysis of thermophoresis phenomenon have neglected the radiation effect treating the low absorbing, emitting particles such as glass beads,  $TiO_2$  and  $MgO$ [7, 8]. The radiative effect on thermophoresis can be significant when the highly absorbing, emitting particles (soot, pulverized coal) are present in a gas-particle mixture as in an internal combustion chamber, heat exchanger and automobile tailpipe[7].

Recently, Yoa et al. have presented the radiation effect on thermophoretic transport of particles in laminar tube flow qualitatively by numerical computation[11, 12]. Moreover, thermophoresis of small particles in combined forced and free convection flows is influenced by the effect of gravity on the hydrodynamics of forced flow in a long vertical flow. Mixed convection very commonly arises in the environment and in technological applications[15, 16].

Up to present, the effect of a buoyancy driven force on the particle transport mechanism has not been analyzed extensively in a mixed convection flow with the radiation.

Thus, a main goal of the present paper is to investigate qualitatively the buoyant and radiative effects on thermophoresis phenomenon in a laminar long vertical tube flow as a parametric study.

### Governing Equations

A two phase(gas-particle) flow system in this work is limited to low particle mass loading at which the particle motion does not affect the gas flow[28]. The Stokes number as a dimensionless criterion for interphase linear momentum exchange is defined by the ratio of particle stopping time to a characteristic flow time[17]. For very small Stokes numbers, one can explicitly neglect the interaction source terms two phases through the interfacial exchange of momentum. In the present study, a two-fluid model would be used since it can easily incorporate with the particle diffusion effects and can be applied to the multi-dimensional flows. The theoretical analysis for thermophoresis phenomenon yields the following expression for the thermophoretic velocity[7].

$$v_T = -\frac{\nu K}{T} \nabla T \quad (1)$$

where  $K$  is the dimensionless thermophoretic coefficient and depends on the regime of flow past the particle described in terms of Knudsen number ( $Kn = \lambda / (d_p/2)$ ) which represents the ratio of molecular mean free path to particle size. In the transition regime where the molecular mean free path is on the order of the particle radius, Derjaguin et al.[3] give the following expression,

$$K = K_t \frac{1 + C_t(\lambda / (d_p/2))(K_p/K_g)}{1 + K_p / (2K_g) + C_t(\lambda / (d_p/2))(K_p/K_g)} \quad (2)$$

where,  $C_t$  is the temperature jump coefficient in the Smoluchowski formula and  $K_t$  is the thermal slip coefficient. The values of these coefficients are 2.16 and 1.17, respectively.

They found a very good agreement with the experimental data with the numerical values of the thermophoretic coefficient  $K$  ranging from about 0.25 to 1.25 for the different types of aerosol particles.

For a simple analysis of the present problem, the following assumptions are introduced.

1. Flow is a dilute gas-particle flow due to the low particle mass loading.
2. At tube inlet, flow fields of each phase are assumed to be uniform.
3. Temperature and particle concentration distributions are uniform at the pipe inlet.
4. Fluid and particle properties are independent of temperature.
5. Pipe wall is isothermal and gray.
6. The gas is transparent to radiation and the solids are limited to the gray absorbing, emitting particle without scattering.
7. The absorption coefficient is constant in all thermal field.
8. Particle coagulation and collision are neglected.
9. The gas and particle phase are in the same temperature.

For the present problem configuration, Fig.(1) is referred. On the basis of a two fluid model, the governing equations of each phase can be written as follows :

#### Gas Phase

$$\frac{\partial u_g}{\partial \xi} + \frac{1}{\eta} \frac{\partial}{\partial \eta} (\eta v_g) = 0 \quad (3)$$

$$\rho_g u_g \frac{\partial u_g}{\partial \xi} + \rho_g v_g \frac{\partial u_g}{\partial \eta} = -\frac{\partial p^*}{\partial \zeta} + \frac{1}{Re_R}$$

$$\left( \frac{\partial^2 u_g}{\partial \zeta^2} + \frac{1}{\eta} \frac{\partial u_g}{\partial \eta} + \frac{\partial^2 u_g}{\partial \eta^2} \right) + \frac{Gr}{Re_R^2} \frac{\theta - \theta_w}{\theta_{in} - \theta_w} \quad (4)$$

$$\rho_g u_g \frac{\partial v_g}{\partial \xi} + \rho_g v_g \frac{\partial v_g}{\partial \eta} = -\frac{\partial p^*}{\partial \zeta} + \frac{1}{Re_R}$$

$$\left( \frac{\partial^2 v_g}{\partial \zeta^2} + \frac{1}{\eta} \frac{\partial v_g}{\partial \eta} + \frac{\partial^2 v_g}{\partial \eta^2} \right) \quad (5)$$

The dimensionless variable are defined as

$$\xi = \frac{x}{R}, \quad \eta = \frac{r}{R}, \quad \theta = \frac{T_g}{T_{in}} \approx \frac{T_p}{T_{in}} \approx \frac{T}{T_{in}} \quad (6)$$

where,  $U_{avg}$  is a characteristic velocity taken as a mean velocity in this study, gas velocity components,  $U_g$  and  $V_g$ , are normalized by  $U_{avg}$ ,  $Re_R = U_{avg} R / \nu_g$  is the Reynold number, and  $Gr = \{g\gamma(T - T_{in})R^3 / \nu_g^2\}$  is the Grashof number.

The boundary conditions for the problem are given by

$$\frac{\partial u_g}{\partial \eta} = 0, \quad v_g = 0 \quad \text{at } \eta = 0$$

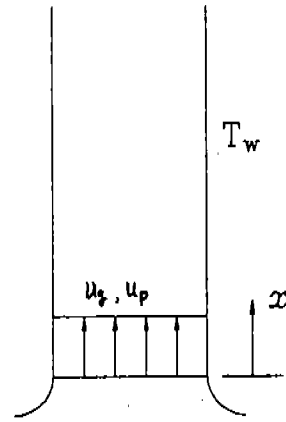
$$u_g = 0, \quad v_g = 0 \quad \text{at } \eta = 1$$

$$u_g = U_{avg}, \quad v_g = 0 \quad \text{at } \zeta = 0$$

$$\frac{\partial^2 u_g}{\partial \zeta^2} = 0, \quad \frac{\partial^2 v_g}{\partial \zeta^2} = 0 \quad \text{at exit} \quad (7)$$

In equation(4), the body force term is included in axial direction for a long vertical tube flow.

For a gas phase, gas density variation is assumed to be negligible except in the buoyancy term of an axial momentum equation(Boussinesq app-



Uniform  $T_{in}$

Fig. 1 Entrance configuration.

roximation). Invoking the Boussinesq approximation, the gas density  $\rho_g$  is defined by

$$\rho_g = \rho_{g, in} [1 - \gamma(T - T_{in})] \quad (8)$$

where,  $\rho_{g, in}$  is the density evaluated at the inlet reference temperature  $T_{in}$  and

$$\gamma = -\frac{1}{\rho_g} \left( \frac{\partial \rho_g}{\partial T} \right) \quad (9)$$

is a coefficient of expansion with respect to temperature.

And a modified pressure  $p^*$  is defined as,

$$p^* = p + \rho_{g, in} g \zeta \quad (10)$$

The pressure gradient and body force terms in the axial momentum equation are

$$\frac{\partial p^*}{\partial \zeta} + \rho_{g, in} g \gamma (T - T_{in}) \quad (11)$$

Particle phase

$$\frac{\partial}{\partial \xi} (\phi u_p) + \frac{1}{\eta} \frac{\partial}{\partial \eta} (\eta \phi v_p) = 0 \tag{12}$$

$$u_p \frac{\partial u_p}{\partial \xi} + v_p \frac{\partial u_p}{\partial \eta} = -\frac{1}{Stk} (u_p - u_g) - \frac{1}{Stk} \frac{K}{Re_R} \frac{1}{\theta} \frac{\partial \theta}{\partial \xi} \tag{13}$$

$$u_p \frac{\partial v_p}{\partial \xi} + v_p \frac{\partial v_p}{\partial \eta} = -\frac{1}{Stk} (v_p - v_g) - \frac{1}{Stk} \frac{K}{Re_R} \frac{1}{\theta} \frac{\partial \theta}{\partial \eta} \tag{14}$$

where,

$$\xi = \frac{x}{R}, \eta = \frac{r}{R}, \phi = \frac{\rho_p}{\rho_p \text{ in}}, \theta = \frac{T}{T_{\text{in}}} \\ Re_R = \frac{U_{avg} R}{v_g}, Stk = \frac{\rho_{pm} d_p^2 U_{avg}}{18 \mu R} \tag{15}$$

The particle velocity components,  $u_p$ , and  $v_p$ , are normalized by  $U_{avg}$ ,  $\rho_p$  denotes the apparent density of dispersed particles defined as  $\rho_p = \rho_{pm} n_p v_p$ . The Stokes number represents the ratio of the momentum relaxation time  $\tau_{mom}$  to the characteristic flow time  $\tau_{flow}$ [17]. If the Stokes number is very small, the particles will move with the host fluid in the same manner. The similar concept can be applied to the thermal relaxation time  $\tau_T$ .  $\tau_{mom}$  coincides with  $\tau_T$  when  $\tau_T$  the Prandtl number is 2/3[18].  $Pr = 2/3$  is used in the present study.

The boundary conditions for the problem are given by

$$u_p = u_g, v_p = 0, \phi = 1 \quad \text{at } \xi = 0 \\ \frac{\partial u_p}{\partial \eta} = v_p = \frac{\partial \phi}{\partial \eta} = 0 \quad \text{at } \eta = 0 \tag{16}$$

Since the particle momentum equations are described by the first order partial differential equations, only the upstream boundary conditions are needed.

The mixture energy equation can be written as[30]

$$(1 + C_L) \left( u_g \frac{\partial \theta}{\partial \xi} + v_g \frac{\partial \theta}{\partial \eta} \right) = \frac{1}{Pe_R} \frac{\partial^2 \theta}{\partial \xi^2} + \frac{1}{Pe_R} \frac{1}{\eta} \frac{\partial}{\partial \eta} \left( \eta \frac{\partial \theta}{\partial \eta} \right) - \frac{\tau_o^2}{Pe_R N} (\theta^4 - G_o) \tag{17}$$

where,

$$C_L = \frac{\rho_p c_{pp}}{\rho_g c_{pg}} \\ Pe_R = Re_R Pr, \tau_o = \beta R \\ N = \frac{K_g \beta}{4 \sigma n^2 T_{in}^3}, G_o = \frac{I_o}{4 \sigma n^2 T_{in}^4} \tag{18}$$

The boundary conditions are given by

$$\theta = 1 \quad \text{at } \xi = 0 \\ \frac{\partial^2 \theta}{\partial \xi^2} = 0 \quad \text{at exit} \\ \frac{\partial \theta}{\partial \eta} = 0 \quad \text{at } \eta = 0 \\ \theta = \theta_w \quad \text{at } \eta = 1 \tag{19}$$

The boundary condition at exit may be justified if a sufficiently long length is used.

The coefficient  $C_L$  is assumed to be in the range less than 0.2 under the assumption of low mass loading and proper heat capacity for the particle phase.

In equation(17), the radiation source term  $G_o$  is obtained from the radiative transport equation for a non-scattering medium employing P-1 approximation method[19-21]. The particle deposition flux to the wall may be expressed as

$$J_p = \phi v_p |_w \quad (20)$$

Also, the cumulative collection efficiency is defined as the percentage of the particles that are deposited on the wall within a distance  $x$  from the tube inlet[8].

$$E(x) = \frac{\int_0^x J_p(s) 2\pi ds}{\phi_{in} U_{avg} \pi R} \quad (21)$$

## Results and Discussion

We obtained the present numerical solutions for the conservation equations by line SOR solver, utilizing the power law differencing scheme and upwind scheme for particle transport. P-1 approximation method is adopted for the radiative transport equation. The accuracy of numerical method is referred to Yoa and Kim's solution[11, 12].

The numerical results are obtained as the dimensionless parameters such as Reynolds number, Grashof number, Prandtl number, optical thickness and conduction to radiation parameter, etc.

Reynolds number is taken as the value of 200 which is not relatively high to maintain the proper  $Gr/Re$  for the simultaneous effects of a combined forced and free convection[22, 23].

Figure 2-a, b, c illustrate the gaseous axial velocity profiles along axial distance in combined forced and free convection flows involving the radiative heat transfer ( $Gr=10000$ ,  $Re=200$ ,  $Pr=1$ ,  $\tau_0=0, 0.5, 1.0$ ,  $N=0.01$ ). For the above dimensionless variables, a natural convection regime may be significant since a natural convection-dominant regime corresponds to  $Gr>30$ . From the experimental investigation by Morton et al[16], it is noted that flows with  $Gr/Re$  of the order of 500 can exhibit the substantial regions of cir-

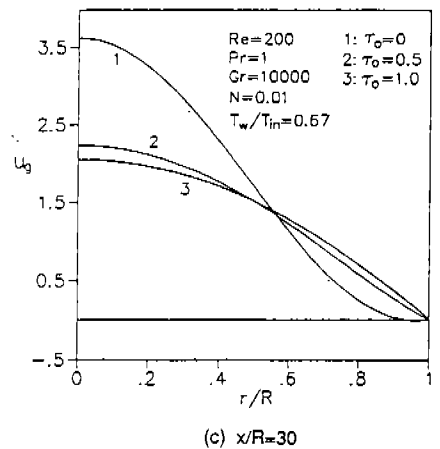
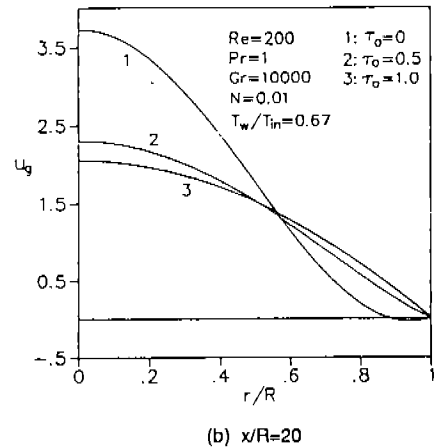
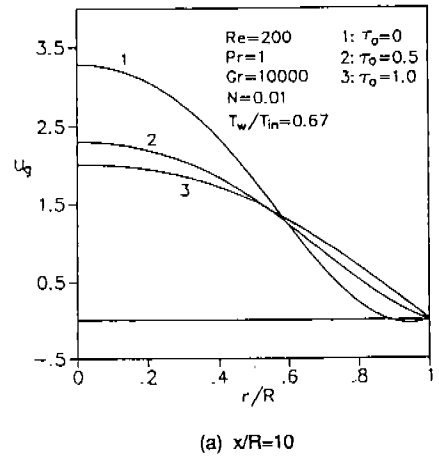
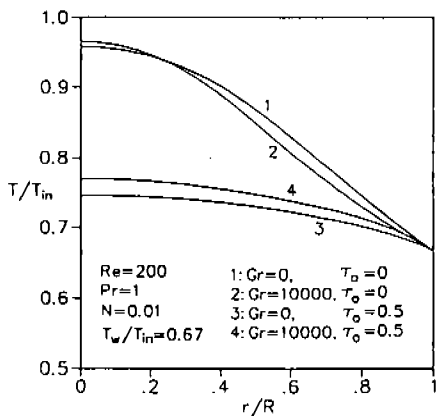
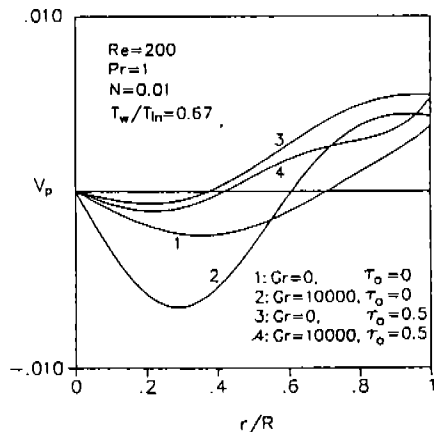


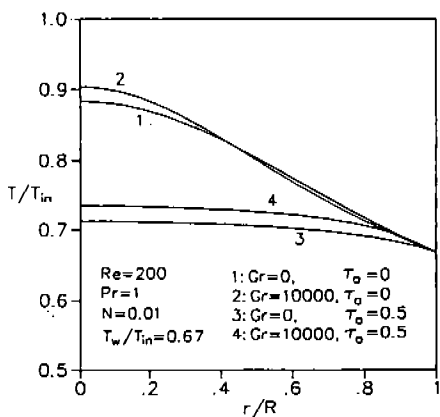
Fig. 2-a, b, c Axial gaseous velocity profiles at various axial distance.



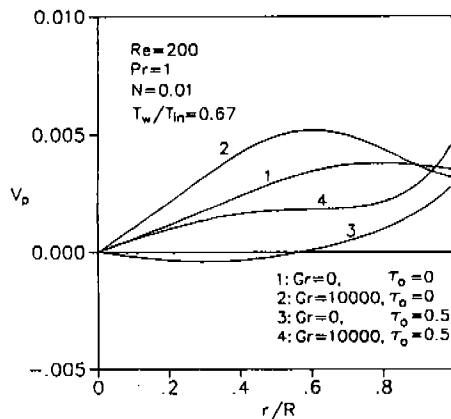
(a)  $x/R=10$



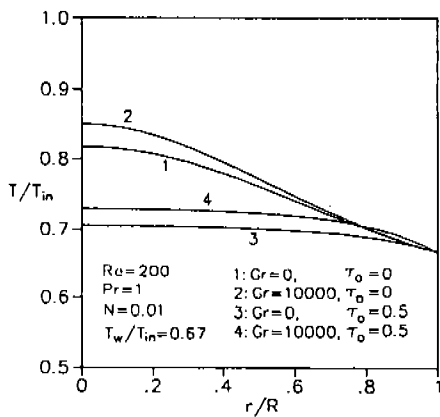
(a)  $x/R=10$



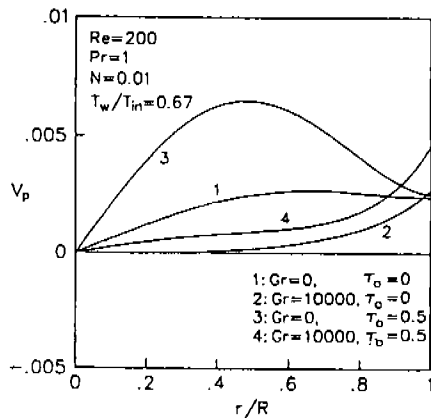
(b)  $x/R=20$



(b)  $x/R=20$



(c)  $x/R=30$



(c)  $x/R=30$

Fig. 3—a, b, c Comparison of temperature distributions at  $Gr=0, 10000$ .

Fig. 4—a, b, c Comparison of radial particle velocity profiles at  $Gr=0, 10000$ .

culating flow. Proceeding downstream ( $x/R \times 20$ ), this effect is getting weaker since the gas temperature approaches the wall temperature. Simultaneously, between  $r/R=0$  and  $0.4$ , due to the effect of gravitational body force, the fluid is to be accelerated and hence the fluid has a peak axial velocity at tube core.

Moreover, for  $\tau_w=0.5$ ,  $1.0$  and  $N=0.01$ , the radiation is an additional mechanism for heat transfer increasing heat flux and radiation source term augments the rate of thermal development; that is, the temperature is decaying at more rapid rate. Thus, the buoyancy effect opposing a forced flow is decreased and this effect is completely ceased moving far downstream.

Figure 3-a, b, c show the temperature profiles at  $Gr=0, 10000$ ,  $Re=200$ ,  $Pr=1$ ,  $\tau_w=0, 0.5$  and  $N=0.01$ . The fluid temperature must decrease in a direction of increasing radius, which  $\gamma > 0$  implies that the fluid density increases. Therefore, the decelerative effect of a gravitational body force, which is proportional to the density, increases in radial direction. With a radiative source term involved in an energy conservation equation, it tends to uniformize the temperature distribution rapidly due to far reaching nature. As the results, it relaxes the effect of a gravitational body force.

Figure 4-a, b, c represent the comparison of the dimensionless velocity  $V_p$  for  $Gr=0, 10000$  at given  $\tau_w=0, 0.5$  and  $N=0.01$ . The Stokes number is defined as.

$$Stk = \frac{\rho_p d_p^2 U_{avg}}{18 \mu R}$$

For small Stokes number directly dependent upon the particle size (small particle size), the particle motion follows that of host fluid sufficiently in the same manner. However, for a gas-particle suspension in a non-isothermal field, small particles acquire the thermophoretic velocity in the direction of decreasing a temperature. In our

present study into domain of negligible inertia we also neglect the drift produced by gas vorticity-induced lift force compared to the prevailing thermophoretic drift velocity across streamlines; that is, the local slip velocity  $V_p - V_g$  is influenced by a thermophoretic velocity. As a consequence, a negative particle radial velocity towards a central core is decreased due to a thermophoretic effect generated by the temperature gradient in a surrounding gas.

As shown in this Figure,  $V_p$  becomes larger than that without this effect in no relation with radiation when the buoyant effect is applied. As discussed in the foregoing, for an opposing flow condition, the axial flow velocity far from the wall becomes accelerated at higher Grashof number, and hence the convected heat transfer is relatively getting larger in comparison with that of wall region. Thus, it results in a larger thermophoretic velocity due to a steeper temperature gradient. With a similar aspect, the value of  $V_p$  at  $\tau_w=0.5$  illustrates smaller  $V_p$  than that at  $\tau_w=0$  for the value of Grashof number since the radiative effect may decrease a natural convection heat transfer mechanism. As flows proceed downstream ( $x/R > 20$ ), due to the more development of flow and decrease of buoyancy effect, except for the wall region, higher  $V_p$  at  $Gr=10000$  is illustrated than that of  $Gr=0$ . When the fluid temperature approaches the wall temperature far downstream, the effect of a gravitational body force ultimately vanishes and the velocity eventually reaches a fully developed parabolic profile. This trend may be established much earlier as a strong radiative effect is considered. Thus, at  $\tau_w=0.5$ , an increase in the buoyancy effect on  $V_p$  is getting weak at more rapid rate and difference of the magnitude of  $V_p$  for both cases ( $Gr=0, 10000$ ) becomes smaller.

Figure 5-a, b, c illustrate the comparison of the particle concentration profiles at  $Gr=0, 10000$  for  $\tau_w=0, 0.5$ . From Fig. 2, as the buoyancy effect



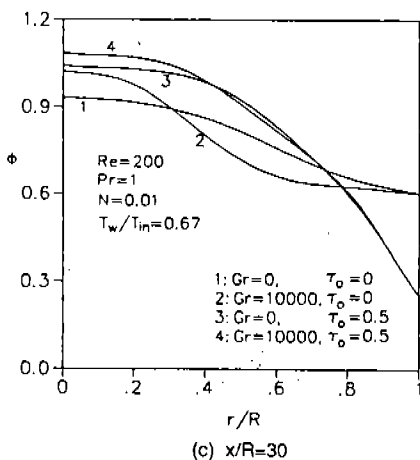
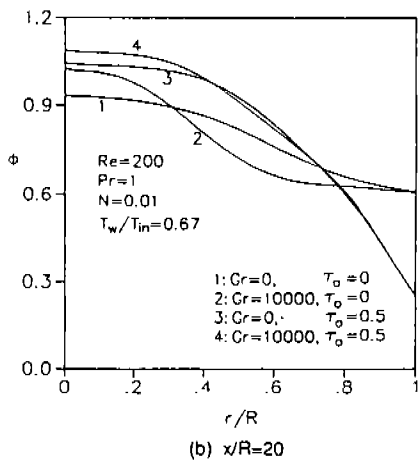
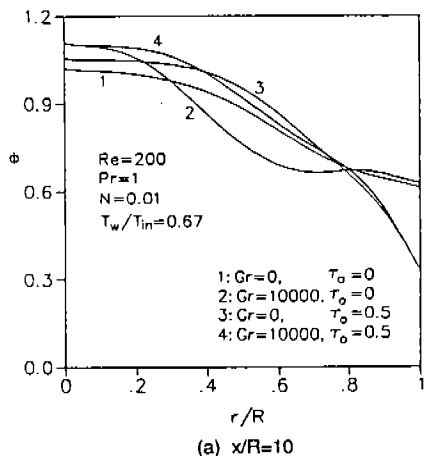


Fig. 5— a, b, c Comparison of particle concentration profiles at  $Gr=0, 10000$ .

opposing a forced flow is taken into account. it is noted that due to a higher fluid acceleration, the particle concentration becomes larger than that of  $Gr=0$  around tube core region. However, considering the radiation effect since the radiation relaxes the effect of a gravitational body force,  $\Phi$  is a bit more increased compared with that of  $Gr=0$  and  $\tau_o=0.5$  for  $0 < r/R < 0.4$ . Moving far downstream, the fluid temperature approaches asymptotically the wall temperature and hence the effect of buoyancy driven particle motion is decreased. As a strong radiation is contributed, this phenomenon may be more significant.

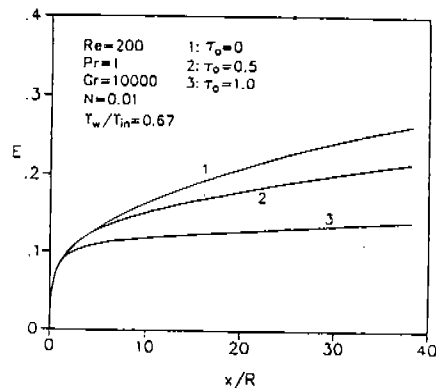


Fig. 6 Cumulative collection efficiency for  $Gr=10000$ , along axial distance.

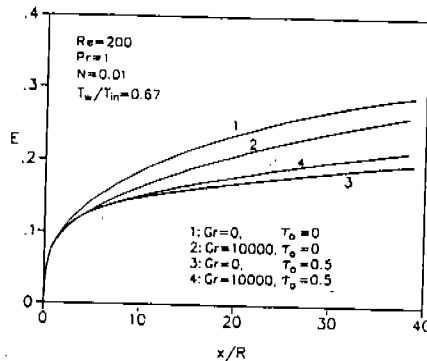


Fig. 7 Comparison of cumulative collection efficiency for  $Gr=0, 10000$  along axial distance.

Figure. 6 gives  $E(x)$  along axial distance at  $Gr=10000$ ,  $Re=200$  for various optical thickness in the case of a combined forced and free convection. In order to investigate the effect of a gravity force in a mixed convection flow on  $E(x)$ , Fig. 7 shows the numerical results of  $Gr=0$ ,  $10000$  under consideration of radiation. As known in Fig. 5 it is found that the value of  $E(x)$  at  $Gr=0$  is a bit smaller than that of  $Gr=10000$  at  $\tau_0=0.5$ . In particular, the temperature distributions of  $Gr=0$ ,  $10000$  at  $\tau_0=0.5$  indicate that a higher temperature gradient at  $Gr=10000$  is illustrated near the wall due to an increase of convective and radiative energy transport except for the wall region compared to that of  $Gr=0$ . As a result, the thermophoretic velocity of  $Gr=10000$  becomes a bit higher than that of  $Gr=0$  at  $\tau_0=0.5$ . It results in a bit higher  $E(x)$  in a mixed convection flow ( $Gr=10000$ ).

### Conclusions

Thermophoresis of small particles in a combined forced and free convection is affected by the effect of a gravitational body force on the hydrodynamic and thermal characteristics of a forced flow in a long vertical tube. Several important observations are noted and summarized below.

Due to the deficiency of experimental evidence, the observations are mainly of qualitative value.

1. In the presence of the buoyancy opposing the main flow, the hydrodynamic and thermal characteristics of host fluid are significantly altered due to the effect of flow reversal.
2. As the buoyancy effect opposing the forced flow is increased, it is noted that the particle concentration becomes larger than that of  $Gr=0$  around tube core, while smaller near the wall.
3. When the radiation is combined with mixed convection, the radiative effect of relaxes the

effect of gravitational body force due to rapid thermal development rate. As a result, the particle concentration is smaller than that without radiation ( $Gr=10000$ ).

4. At  $\tau_0=0$ , the cumulative collection efficiency of  $Gr=10000$  is decreased compared with that of  $Gr=0$ . As the strong radiation is contributed, the value of  $E(x)$  at  $Gr=10000$  becomes a bit larger than that at  $Gr=0$  due to a steeper temperature gradient in the vicinity of the wall.

### References

1. Batchelor G.K. and Shen C. "Thermophoretic deposition of particles in gas flowing over cold surfaces." *J. Colloid and Interface Science*, Sep., 1985, vol.107(1), 21-37.
2. Fulford G.D., Moo-Young M., and Bebu M., "Thermophoretic Acceleration of Particle Deposition from Laminar Air Streams" *Canad. J. Chem. Eng.* 49, 553(1971)
3. Derjaguin B.V., Rabinovich Ya. I., Storozhilova A.I., and Shcherbina G.I., "Measurement of the Coefficient of Thermal Slip of Gases and the Thermophoresis Velocity of Large-Size Aerosol Particles" *J. Colloid and Interface Science*, Vol.57, 451 (1976)
4. Goldsmith P., and May F.G., "Aerosol Science". Academic Press, New York, 1966.
5. Rosner D.E. and Kim S.S., *Chem. J.*, 29, 1984.
6. Calvert S. and Byers L.J. "Air Pollution Control Assoc." vol.17, 595(1967)
7. Goren S.L. "Thermophoresis of Aerosol Particles in the laminar Boundary Layer on a Flat Plate", *J. Colloid and Interface Science*, Vol.61, No.1, August (1977)
8. Walker K.L., Homesy G.M. and Geyling F.T. "Thermophoretic Deposition of Small Particles in Laminar Tube Flow" *J. Colloid and Interface Science*, Vol.69, March (1979)

9. Morse T.F., Wang C.Y. and Cipolla J.W. "Laser-Induced Thermophoresis and Particulate Deposition Efficiency" ASME, J. Heat Transfer, Vol.107, Feb. 1985.
10. Cipolla J.W. and Morse T.F. "Thermophoresis in an Absorbing Aerosol" J. Aerosol Science, Vol.18, No.3, pp.245-260, 1987.
11. Yoa S.J., Kim S.S., and Lee J.S. "Thermophoresis of highly absorbing, emitting particle in laminar tube flow ; Int. J. heat and Fluid Flow, vol.11, No.2, June (1990)
12. Yoa S.J. and S.S. : "Numerical study on thermophoretic deposition of highly absorbing, emitting particles suspended in a non-isothermal two-phase flow system" 한국자동차 공학회지, 11권 5호, 1989, 10.
13. Gebhart B., Jaluria Y., Mahajan R.L., and Sammakia B. "Buoyancy-Induced Flows and Transport" Springer-Verlag, 1988.
14. Law Hin-Sum, Masliysah, and Nandakumar K. "Effect of Nonuniform Heating on Laminar Mixed Convection in Ducts" ASME, J. Heat Transfer, Feb, 1987, Vol.109, 131-137.
15. Choudhury D. and Patankar S.V. "Combined Forced and Free Laminar Convection in the Entrance Region of an Inclined Isothermal Tube" ASME, J. Heat Transfer, Nov 1988, Vol.110, 901-909.
16. Morton B.R., Ingham D.B., Keen D.J., and Hegggs P.J. "Recirculating Combined Convection in Laminar Pipe Flow" ASME, J. Heat Transfer, Feb 1989, 106-113.
17. Crowe C.T. "Review-Numerical methods for Dilute Gas-Particle Flow" ASME, J. Fluid Engineering, Vol.104, September 1982.
18. Marble F.E. "Dynamics of dusty gases." Ann. Review, Fluid Mech., 1970, Vol.2, 397-446.
19. Higennyi J. and Bayazitoglu Y. "Differential Approximation of Radiative Heat Transfer in a Gray Medium" ASME, J. Heat Transfer, Vol.102, November 1980.
20. Ratzel A.C. and Howell J.C. "Two-dimensional Radiation in Absorbing Emitting Media Using the P-N Approximation" ASME, J. Heat Transfer, Vol.105, May 1983.
21. Menguc M.P. and Viskanta R. "Radiative Transfer in Axisymmetric, Finite Cylindrical Enclosures" ASME, J. Heat Transfer, Vol.108, May 1986.
22. Chow L.C., Husain S.R., and Campo A. "Effects of Free Convection and Axial Conduction on Forced-Convection Heat Transfer Inside a Vertical Channel at Low Peclet Numbers" ASME, J. Heat Transfer, May 1984, Vol.106, 297-303.
23. Benjan A. "Convective Heat Transfer" A wiley-Interscience Publication, 1984.